

# Subdivision Schemes for Variational Splines

Joe Warren    Henrik Weimer

*Department of Computer Science, Rice University, Houston, TX 77251-1892*

*{jwarren,henrik}@rice.edu*

---

## Abstract

The original theory of splines grew out of the study of simple variational problems. A spline was a function that minimized some notion of energy subject to a set of interpolation constraints. A more recent method for creating splines is subdivision. In this framework, a spline is the limit of a sequence of functions, each related by some simple averaging rule. This paper shows that the two ideas are intrinsically related. Specifically, the solution space to a wide range of variational problems can be captured as spline spaces defined through subdivision.

*Keywords:* geometric modeling; variational design; subdivision

---

## 1 Introduction and Motivation

A fundamental problem in geometric design is the representation of smooth shapes with mathematical models. The general theme of variational design is to define a shape as the minimizer of some energy functional. For example, B-Splines minimize a simple approximation of bending energy. The aim of this paper is to exhibit the intrinsic link between subdivision and variational design.

We show that the solution spaces for the most common class of variational problems have an interesting nesting property. This in turn implies that subdivision can be used to express minimizing solutions. We exhibit a methodology for deriving subdivision schemes whose limit shapes are minimizers of variational problems.

### 1.1 *Natural Cubic Splines*

Historically, a spline was a thin, flexible piece of wood used in drafting. The draftsman attached the spline to a sequence of anchor points on a drafting table. The

spline was then allowed to slide through the anchor points and assume a smooth, minimum energy shape.

In the 1940's and 50's, mathematicians realized that the behavior of a spline could be modeled mathematically. Let the shape of the spline be modeled by the graph of a function  $F(t)$  over a domain interval  $[a, b]$ . The first derivative  $F'(t)$  gives the tangents for  $F(t)$ . Thus, the second derivative  $F''(t)$  measures how much the tangents of  $F$  change. In other words,  $F''(t)$  indicates how much  $F(t)$  bends at  $t$ . Therefore, the bending energy at parameter value  $t \in [a, b]$  is roughly proportional to the value of the second derivative of  $F$  with respect to  $t$ . The total bending energy associated with the function  $F$  on the interval  $[a, b]$  can be approximated by the integral of the square of the second derivative of  $F$ ,

$$\mathcal{E}[F] = \int_a^b F_{tt}(t)^2 dt. \quad (1)$$

The effects of the anchor points on the spline are modeled by constraining  $F$  to satisfy additional interpolation conditions. If  $T_0$  denotes a vector of parameter values for these interpolation conditions,  $T_0 = t_0, t_1, \dots, t_n$  and  $c_0$  denotes a vector of interpolation values, then these conditions can be stated more concisely in vector notation as

$$F(T_0) = c_0. \quad (2)$$

The entries of  $T_0$  are also called *knots* and  $T_0$  is called the *knot vector*. Functions that minimize (1) and satisfy (2) are called *Natural Cubic Splines*<sup>1</sup>.

## 1.2 Variational Problems

More generally, a variational problem is defined over a domain  $\Omega$  that is a closed subset of  $\mathbb{R}^d$ . Let the  $T_k$  be a nested sequence of knot sets  $T_k \subseteq \Omega$  such that  $T_k \subset T_{k+1}$ . The knot sets  $T_k$  are assumed to grow dense in  $\Omega$  as  $k \rightarrow \infty$ . The interpolation conditions for the variational problem are enforced over  $T_0$ , the initial knot set.

**Definition 1** Given an inner product of the form

$$\langle F, G \rangle = \int_{\Omega} \sum_i k_i (\mathcal{D}_i F(t)) (\mathcal{D}_i G(t)) dt \quad (3)$$

<sup>1</sup> As we will point out later, any  $F$  minimizing (1) has zero second derivative at the respective endpoints, i.e.  $F''(t_0) = F''(t_n) = 0$ .

where the  $\mathcal{D}_i$  are differential operators of order  $m$  we define an associated energy functional  $\mathcal{E}[F] = \langle F, F \rangle$  with

$$\mathcal{E}[F] = \int_{\Omega} \sum_i k_i (\mathcal{D}_i F(t))^2 dt. \quad (4)$$

A variational spline is a function  $F(t)$  that minimizes  $\mathcal{E}[F]$  subject to the condition that  $F(t)$  interpolates a given set  $c_0$  of values at  $T_0$ , i.e.  $F(T_0) = c_0$ . For this minimization problem to be well-defined, the constants  $k_i$  are required to be positive. Equation (4) is also called an elliptic, self-adjoint variational problem.

Typically, the space of possible solutions  $F$  is restricted to those functions for which  $\mathcal{E}$  is well-defined. If  $L_2(\Omega)$  denotes those functions that are square integrable over  $\Omega$ , then let  $H_m(\Omega)$  denote those functions for whom all derivatives of up to order  $m$  are in  $L_2(\Omega)$ . By this definition,  $\mathcal{E}[F]$  is defined for all  $F \in H_m(\Omega)$ . The spaces  $H_m(\Omega)$  are the standard Sobolev spaces  $W_2^m(\Omega)$  used in finite element analysis (see Oden and Reddy [OR76] for more details).

Note that in the definition of the energy functional (4) all differential operators  $\mathcal{D}_i$  are of the same order  $m$  and squared, i.e. the problem is elliptic and self-adjoint. Elliptic, self-adjoint variational problems are very common. The Euler-Lagrange equations provide a link between variational problems given in terms of an energy functional  $\mathcal{E}$  and a partial differential equation. For elliptic, self-adjoint variational problems the corresponding partial differential equations are linear and the minimizers are unique and well-defined [OR76].

If  $\mathcal{D}_*$  is the homogeneous differential operator of order  $2m$

$$\mathcal{D}_* = \sum_i k_i (\mathcal{D}_i)^2,$$

then the minimizing  $F(t)$  for equation (4) satisfies two equations

$$\begin{aligned} \mathcal{D}_* F(t) &= 0 & \forall t \in \Omega - T_0, \\ F(T_0) &= c_0 & \forall t \in T_0. \end{aligned} \quad (5)$$

In the literature, the upper partial differential equation is also called the *strong form* of equation (4) and can be derived via the Euler-Lagrange equations.

**Example 2** *Natural Cubic Splines are an elliptic, self-adjoint variational problem. Given domain  $\Omega \subset \mathbb{R}$  the associated inner product is*

$$\langle F, G \rangle = \int_{\Omega} F_{tt}(t) G_{tt}(t) dt. \quad (6)$$

Thus, the energy functional  $\mathcal{E}$  is given by

$$\mathcal{E}[F] = \langle F, F \rangle = \int_{\Omega} F_{tt}(t)^2 dt. \quad (7)$$

According to equation (5), Natural Cubic Splines satisfy the differential equation

$$F_{tttt}(t) = 0 \quad \text{for all } t \in \Omega - T_0 \quad (8)$$

for some knot vector  $T_0 = t_i$  (a common choice for  $T_0$  are the integers from 0 to  $n$ ). Thus, the Natural Cubic Spline  $F$  is actually a piecewise cubic polynomial function. The breaks between the polynomial pieces occur at the parameter values for the interpolation conditions,  $t_i$ .

The derivations in this paper do not make any use of the knowledge about the solution to a particular variational problem being polynomial. In fact, the goal will be to express the minimizers in terms of subdivision without ever relying on an explicit basis for the solution space.

Simple examples of elliptic, self-adjoint variational problems in two dimensions are Harmonic Splines and Polyharmonic Splines, which are defined as the minimizers of  $\int (f_u^2 + f_v^2) dudv$  and  $\int (f_{uu}^2 + 2f_{uv}^2 + f_{vv}^2) dudv$ , respectively. Harmonic Splines will be discussed further in a later section of this paper.

### 1.3 Associated Nested Spaces

As the interpolation values  $c_0$  vary over a fixed knot set  $T_0 \subset \Omega$ , the minimizing solutions  $F(t)$  for an elliptic, self-adjoint variational problem form a linear space  $V(T_0)$ .

**Theorem 3** *Given an elliptic, self-adjoint variational problem  $\mathcal{E}$  and knot set  $T_0 \subset \Omega$  for domain  $\Omega$ , the space of minimizers*

$$V(T_0) = \{F \mid \mathcal{E}[F] \text{ is minimal, and } F(T_0) = c_0 \text{ for some } c_0\}$$

*is linear.*

**Proof:** Because  $\mathcal{E}$  is elliptic and self-adjoint, minimizers of  $\mathcal{E}$  have to satisfy a linear partial differential equation as given by Euler-Lagrange. Now, because differentiation is a linear operation, the sum of two minimizers as well as a scalar multiple of a minimizer are minimizers themselves.  $\square$

**Example 4** Given fixed knot set  $T_0 = \{0, 1, 2, 3, 4\}$  and interpolation conditions  $c_0^1 = \{0, 2, 2, 3, 1\}$  and  $c_0^2 = \{1, 1, 0, 0, 2\}$  we can solve for the corresponding Natural Cubic Splines  $s_1(t)$  and  $s_2(t)$  shown in the top row of figure 1. Solving for the spline satisfying the interpolation condition  $c_0^1 + c_0^2 = \{1, 3, 2, 3, 3\}$  yields the function  $s_1(t) + s_2(t)$  depicted in the bottom of figure 1.

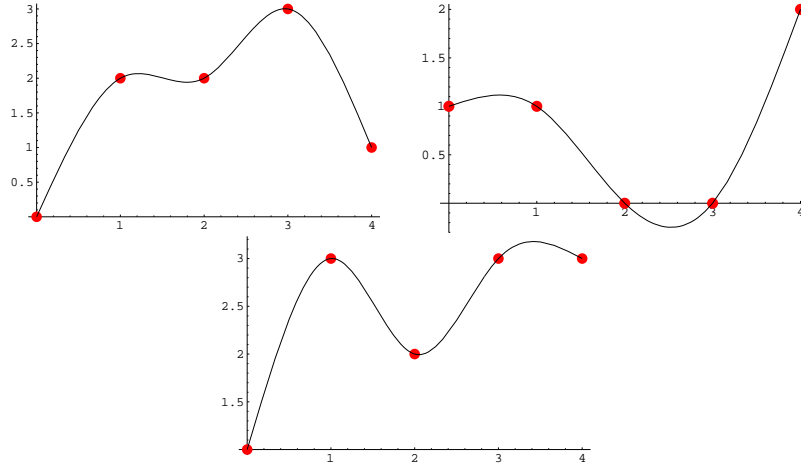


Fig. 1. Adding the spline functions for two interpolation conditions yields the spline for the sum of the interpolation conditions.

**Theorem 5** Let  $V(T_0)$  and  $V(T_1)$  be the spaces of minimizers of an elliptic, self-adjoint variational problem  $\mathcal{E}$  over knot sets  $T_0$  and  $T_1$  respectively. Then,

$$T_0 \subset T_1 \Rightarrow V(T_0) \subset V(T_1).$$

**Proof:** Given any  $F(t) \in V(T_0)$  consider  $\hat{F}(t) \in V(T_1)$  with  $\hat{F}(T_1) = F(T_1)$ . Assuming  $\mathcal{E}[F] > \mathcal{E}[\hat{F}]$  yields a contradiction to  $\mathcal{E}[F]$  being minimal because  $\hat{F}(T_0) = F(T_0)$  and  $\hat{F}$  has smaller energy, i.e.  $F \notin V(T_0)$ . Conversely, assuming  $\mathcal{E}[F] < \mathcal{E}[\hat{F}]$  contradicts  $\mathcal{E}[\hat{F}]$  being minimal because  $F$  itself interpolates  $F(T_1)$ , i.e.  $\hat{F} \notin V(T_1)$ . Therefore,  $\mathcal{E}[F] = \mathcal{E}[\hat{F}]$  and thus  $F = \hat{F}$ .  $\square$

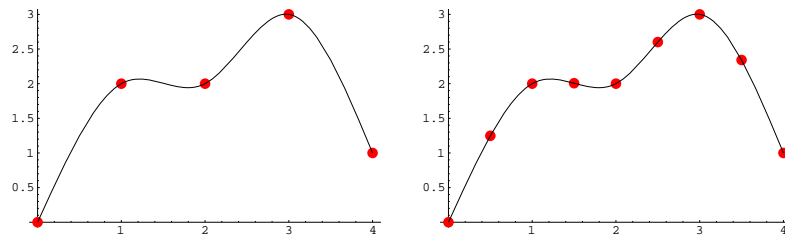


Fig. 2. Nesting of the solution spaces for Natural Cubic Splines.

**Example 6** Solving for the Natural Cubic Spline over the knots  $T_0 = \{0, 1, 2, 3, 4\}$  satisfying the interpolation conditions  $c_0 = \{0, 2, 2, 3, 1\}$  yields the function depicted on the left of figure 2. Sampling this function at the refined knot set  $T_1 = \{0, \frac{1}{2}, 1, \frac{3}{2}, 2, \frac{5}{2}, 3, \frac{7}{2}, 4\}$  and solving for the corresponding spline yields the identical function, depicted at the right of the figure.

## 1.4 Associated Subdivision Scheme

The nesting of the finer and finer solution spaces as described by theorem 5 implies that solutions can be linked through subdivision. The key observation here is that a basis for the coarse space can be expressed in terms of the basis for the next finer space. Subdivision can be seen as a change of basis from a coarse to the next finer basis.

**Theorem 7** *Let  $N_0(t)$  and  $N_1(t)$  be vectors of basis functions for the solution spaces  $V(T_0)$  and  $V(T_1)$  of elliptic, self-adjoint variational problem  $\mathcal{E}$  respectively. Then (in vector notation)*

$$V(T_0) \subset V(T_1) \Rightarrow N_0(t) = N_1(t)S_0$$

for some matrix  $S_0$ , called a subdivision matrix.

**Proof:**  $N_0$  is a basis for  $V(T_0)$ . As  $V(T_0) \subset V(T_1)$ ,  $N_0 \subset V(T_1)$ . As  $N_1$  is basis for  $V(T_1)$ ,  $N_0$  can be represented in terms of this basis. A column of  $S_0$  contains the coefficients for the basis functions in  $N_1$  to represent one particular function in  $N_0$ .  $\square$

Note that the proof of theorem 7 did not require any knowledge about the nature of the bases  $N_i$ . In particular it is not necessary for the bases to be polynomial or piecewise polynomial. Any function  $F(t) \in V(T_0)$  can be represented in terms of the basis  $N_0(t)$  as  $F(t) = N_0(t)p_0$  for some vector of coefficients,  $p_0$ . Due to the nesting of the spaces  $V(T_0) \subset V(T_1)$ ,  $F(t)$  can also be expressed in terms of the basis  $N_1(t)$  for  $V(T_1)$ ,  $F(t) = N_1(t)p_1$ . Because  $N_0(t) = N_1(t)S_0$  it is possible to express the coefficients  $p_1$  of  $F(t)$  in terms of the coefficients  $p_0$  as

$$p_1 = S_0 p_0.$$

The matrix  $S_0$  is called a *subdivision matrix* and naturally links solutions over a coarse knot set to solutions over the next finer set of knots.

**Example 8** *The cubic B-Spline basis [dB72a,Boe80,Far88,HL93] is the basis for Natural Cubic Splines with minimal support. It has been studied to a great extent and was successful in many real world applications. The subdivision scheme for uniform cubic B-Splines is given by the well known Lane-Riesenfeld algorithm*

[LR80]. For example,

$$S_0 = \frac{1}{8} \begin{pmatrix} 8 & 0 & 0 & 0 & 0 \\ 4 & 4 & 0 & 0 & 0 \\ 1 & 6 & 1 & 0 & 0 \\ 0 & 4 & 4 & 0 & 0 \\ 0 & 1 & 6 & 1 & 0 \\ 0 & 0 & 4 & 4 & 0 \\ 0 & 0 & 1 & 6 & 1 \\ 0 & 0 & 0 & 4 & 4 \\ 0 & 0 & 0 & 0 & 8 \end{pmatrix}$$

is the subdivision matrix which maps five control coefficients of a uniform cubic B-Spline into nine finer coefficients. Remaining subdivision matrices have a similar structure: there are two special columns for each boundary of the grid and interior columns of  $S_k$  are all shifts of the column  $\{\dots, 0, 1, 4, 6, 4, 1, 0, \dots\}$ . Figure 3 shows an example application of this subdivision scheme.

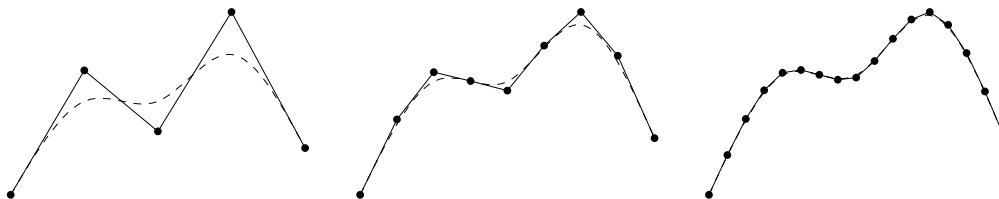


Fig. 3. Subdivision for Natural Cubic Splines.

The main goal of this paper is the derivation of subdivision schemes which produce solutions for elliptic, self-adjoint variational problems. A detailed discussion of the mathematical properties of this approach has been deferred to a technical report [War98].

Methods for variational subdivision have been suggested earlier by Kobbelt et al. [Kob96,KS97,KCVS98]. These subdivision schemes are interpolating, i.e. the limit surfaces go through the initial control points. They require iterative solving for new control coefficients in every round of the subdivision process. The schemes are not as highly localized as the subdivision schemes presented in this paper.

We feel that our work is also significantly related to publications by Dyn [Dyn87], [Dyn86]. The author observes that the linear systems that arise during surface fitting with radial basis functions are numerically very poorly conditioned and that preconditioning the system with an appropriate difference operator yields a numerically much more stable problem. In effect, this corresponds to a change of basis from radial basis functions to a more bell-shaped basis. The subdivision schemes presented here reproduce these bell-shaped basis functions for uniform knot sequences (section 3).

## 2 Finite Element Solution

This section presents a derivation of solutions for elliptic, self-adjoint variational problems in terms of a finite element process.

A finite element method systematically builds better and better approximations to the true minimizer of a variational problem considering a nested sequence of domain grids  $T_k$ . Using a vector of basis functions  $B_k(t)$ , a space of functions  $\text{Span}\{B_k(t)\}$  is associated with every domain grid  $T_k$ . In each of these spaces, the finite element method finds a best approximation  $F_k \in \text{Span}\{B_k(t)\}$  to the true minimizer of the variational problem.

As we shall see later, convergence of the  $F_k$  to the true minimizer of the variational problem can be guaranteed if the sequence of domain grids  $T_k$  and the corresponding finite element bases  $B_k(t)$  are chosen carefully. In fact, even the coefficients  $p_k$  converge to the true minimizer of the variational problem if the finite element bases are chosen well.

Given a domain grid  $T_k$ , solving a variational problem with finite elements involves three major steps:

- Choose a finite element basis  $B_k(t) = \{b_i^k\}$  and define functions of level  $k$  as  $F_k(t) = B_k(t) p_k$ . Here  $p_k$  denotes a vector of coefficients of level  $k$ , providing one coefficient per knot in the domain grid  $T_k$ .
- Measure the energy of  $F_k(t)$  via  $\mathcal{E}[F_k] = p_k^T E_k p_k$  where  $E_k$  turns out to be a symmetric, positive definite matrix.
- Determine the  $p_k$  such that  $F_k(t)$  has minimal energy  $\mathcal{E}[F_k] = p_k^T E_k p_k$  and satisfies the interpolation condition  $F_k(T_0) = c_0$ .

The following sections discuss these steps in more detail.

### 2.1 Finite Element Basis

In terms of finite elements, a best approximation to the solution of the variational problem over the knot set  $T_k$  is defined using a set of continuous basis functions  $B_k(t) = \{b_i^k(t)\}$ , providing one basis function per knot in  $T_k$ .

Using these basis functions, our goal is to determine a best approximation  $F_k(t)$  to the true minimizer of the variational problem, given by

$$F_k(t) = B_k(t) p_k . \tag{9}$$

Here  $p_k$  is a set of unknown coefficients.



Obviously, for the energy  $\mathcal{E}[F_k] = \mathcal{E}[B_k(t)p_k]$  in (4) to be well defined, the basis functions  $B_k(t)$  should have square integrable derivatives up to order  $m$ , i.e. they should lie in the corresponding Sobolev space  $H_m(\Omega)$ .

For reasons of computational stability and simplicity the basis functions should be centered over the knots, e.g. for level 0 the  $i$ -th basis function should have maximum magnitude over the knot  $t_i \in T_0$ .

Convergence of the sequence of finite element solutions  $F_k(t)$  to the true minimizer of the variational problem depends on two factors: First, the aspect ratio of the simplices in the domain discretization  $T_k$  has to be bounded by one constant  $c$ . Second, the finite element basis functions  $B_k$  have to span sufficiently large, complete spaces of polynomials. More detail to the convergence results will be filled in later.

**Example 9** *Due to the structure of the variational problem for Natural Cubic Splines the finite element basis functions have to have square integrable derivatives up to order two. A possible choice for these basis functions are quadratic piecewise Bézier curves.*

*At the boundaries of  $\Omega = [0, 4]$ , we desire basis functions that have linear precision and minimal support. Given these constraints, we propose a piecewise quadratic basis with knots at the half integers. Each of the five rows of numbers in figure 4 are the Bernstein basis coefficients for one of the piecewise quadratic basis functions. (Divide by eight to get the normalized coefficients.)*

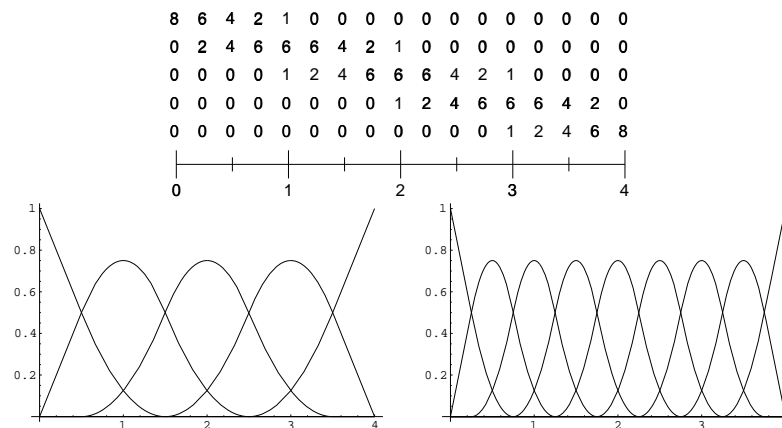


Fig. 4. Bézier control coefficients for the finite element basis functions of level 0 (top) and finite element basis of level 0 and 1 over the domain  $[0, 4]$  (bottom). The basis functions are piecewise quadratic Bézier curves and are centered over the knots.

*For the original grid  $T_0 = \{0, 1, 2, 3, 4\} \subset \Omega = [0, 4]$ , the Bézier control coefficients for the finite element basis  $B_0(t)$  are shown in the top of figure 4 together with the resulting basis functions for level 0 and 1 at the bottom. Finite element basis functions for finer grids are derived similarly using a uniformly refined knot set.*

## 2.2 Energy Matrix and Inner Product

Using the representation  $F_k(t)$  from (9) of the level  $k$  solution of the finite element process, the energy of  $p_k$  can be assessed as  $\mathcal{E}[F_k]$ . This can be expressed as a quadratic form

$$\mathcal{E}[F_k] = p_k^T E_k p_k . \quad (10)$$

where  $E_k$  is a symmetric, positive definite matrix called the *energy matrix* with row and column indices corresponding to knots in  $T_k$ . Using the inner product  $\langle \cdot, \cdot \rangle$  associated with the variational problem (3) we get  $(E_k)_{ij} = \langle b_i^k(t), b_j^k(t) \rangle$ . The result of applying the energy matrix  $E_k$  to a set of coefficients  $p_k$  is called *differences*.

**Example 10** For Natural Cubic Splines, the inner product is given by (6). The energy matrix  $E_0$  based on the piecewise Bézier finite element basis functions from above is

$$E_0 = \begin{pmatrix} 1 & -2 & 1 & 0 & 0 \\ -2 & 5 & -4 & 1 & 0 \\ 1 & -4 & 6 & -4 & 1 \\ 0 & 1 & -4 & 5 & -2 \\ 0 & 0 & 1 & -2 & 1 \end{pmatrix} .$$

Subsequent finite element bases  $B_k(t)$  can be derived from the initial basis  $B_0(t)$  by adding new uniform basis functions to the interior of  $\Omega$ . The corresponding energy matrices  $E_k$  are uniform on the interior of  $\Omega$  and agree with  $E_0$  on the boundary of  $\Omega$ . Note that the  $E_k$  should be scaled by an extra factor of  $\delta^k$  to reflect the change in the grid spacing on the second derivative ( $16^k$ ) and the integral ( $\frac{1}{2^k}$ ) in (1).

## 2.3 Minimization with Interpolated Values

For  $\mathcal{E}[F_k]$  to be minimal, the control points  $p_k$  have to minimize  $p_k^T E_k p_k$  subject to the interpolation conditions  $F_k(T_0) = c_0$ . In this section, we set up the linear system resulting from this problem and solve for the unknown coefficients  $p_k$ .

Due to the interpolation constraints,  $p_k$  is not completely unknown. Some of the entries in  $p_k$  correspond to the knots  $T_0$  with interpolation conditions  $c_0$ . In fact,  $p_k$  can be partitioned into a known part  $p_k^n$  and an unknown part  $p_k^u$  as

$$p_k = \begin{pmatrix} p_k^n \\ p_k^u \end{pmatrix}$$

where  $p_k^n$  contains coefficients centered over the knots  $T_0$  and  $p_k^u$  corresponds to the knots  $T_k - T_0$ .

Using this decomposition of  $p_k$ , equation (10) can be restated as

$$\begin{aligned}\mathcal{E}[F_k] &= p_k^T E_k p_k \\ &= (p_k^{nT} \ p_k^{uT}) \begin{pmatrix} E_k^{nn} & E_k^{nu} \\ E_k^{un} & E_k^{uu} \end{pmatrix} \begin{pmatrix} p_k^n \\ p_k^u \end{pmatrix} \\ &= p_k^{nT} E_k^{nn} p_k^n + 2p_k^{uT} E_k^{un} p_k^n + p_k^{uT} E_k^{uu} p_k^u.\end{aligned}\tag{11}$$

$E_k^{nn}$  contains those entries of  $E_k$  which have row and column indices corresponding to known grid values (knots in  $T_0$ ),  $E_k^{un}$  contains entries of  $E_k$  which have row indices of unknown and column indices of known coefficients (row indices of knots in  $T_k - T_0$  and column indices of knots in  $T_0$ ) and so on.

Now,  $p_k^{nT} E_k^{nn} p_k^n$  is constant,  $2p_k^{uT} E_k^{un} p_k^n$  is linear, and  $p_k^{uT} E_k^{uu} p_k^u$  is a quadratic form in the unknowns  $p_k^u$ . Therefore, the derivative of (11) with respect to the unknowns  $p_k^u$  can be expressed as  $2E_k^{un} p_k^n + 2E_k^{uu} p_k^u$  and the minimizer of (10) is the solution  $p_k^u$  to

$$E_k^{uu} p_k^u + E_k^{un} p_k^n = 0.\tag{12}$$

Using block matrix notation, equation (12) can be rewritten as

$$\begin{pmatrix} E_k^{uu} & E_k^{un} \end{pmatrix} \begin{pmatrix} p_k^u \\ p_k^n \end{pmatrix} = 0.$$

Incorporating the interpolation constraints yields

$$\begin{pmatrix} E_k^{uu} & E_k^{un} \\ I_k^u & I_k^n \end{pmatrix} \begin{pmatrix} p_k^u \\ p_k^n \end{pmatrix} = \begin{pmatrix} 0 \\ \mathcal{I} \end{pmatrix} c_0,\tag{13}$$

where  $(I_k^u I_k^n)$  is the interpolation matrix of level  $k$  for the finite element basis chosen, i.e.  $(I_k^u I_k^n) \begin{pmatrix} p_k^u \\ p_k^n \end{pmatrix}$  yields the value  $F_k(T_k)$  of the finite element representation  $F_k(t) = B_k(t)p_k$  over the knots  $T_k$ .  $\mathcal{I}$  denotes the identity matrix on  $T_0$ .

From the finite element literature [Sha95] we know that the convergence of the interpolating finite element solution (13) is governed by two factors: The space of polynomials spanned by the finite element basis used and the aspect ratio of the finite elements. For more details the interested reader is referred to Chapter 3 of [Sha95].

**Theorem 11** *If the finite element basis functions used for the construction of the energy matrix  $E_k$  in (10) span the space of polynomials of degree  $r$  and if the aspect ratio of the finite elements at any level is bounded by a constant  $c$ , then the solutions  $\begin{pmatrix} p_k^n \\ p_k^n \end{pmatrix}$  to (13) converge at rate  $O(ch^{r+1})$  where  $h$  denotes the grid spacing.*

**Proof:** See Theorem 3.1, p. 77 in [Sha95].  $\square$

**Example 12** *The finite element basis functions for Natural Cubic Splines are piecewise quadratic polynomials, thus  $r = 2$  in theorem 11. If the knot sets  $T_k$  are derived using uniform refinement of the original knots  $T_0$ , then the aspect ratio of the finite elements is one at any level, i.e.  $c = 1$  in theorem 11. Thus, the interpolating finite element process (13) for Natural Cubic Splines converges at rate  $O(h^3)$ .*

*In this case, the interpolation matrix  $I$  has interior rows that are translates of the sequence  $\frac{1}{8}\{\dots, 0, 1, 6, 1, 0, \dots\}$ . As an example, the system (13) for the grid  $T_1 = \{0, \frac{1}{2}, 1, \frac{3}{2}, 2, \frac{5}{2}, 3, \frac{7}{2}, 4\}$  has the form*

$$\begin{pmatrix} 5 & 1 & 0 & 0 & -2 & -4 & 0 & 0 & 0 \\ 1 & 6 & 1 & 0 & 0 & -4 & -4 & 0 & 0 \\ 0 & 1 & 6 & 1 & 0 & 0 & -4 & -4 & 0 \\ 0 & 0 & 1 & 5 & 0 & 0 & 0 & -4 & -2 \\ 0 & 0 & 0 & 0 & 1 & 0 & 0 & 0 & 0 \\ \frac{1}{8} & \frac{1}{8} & 0 & 0 & 0 & \frac{3}{4} & 0 & 0 & 0 \\ 0 & \frac{1}{8} & \frac{1}{8} & 0 & 0 & 0 & \frac{3}{4} & 0 & 0 \\ 0 & 0 & \frac{1}{8} & \frac{1}{8} & 0 & 0 & 0 & \frac{3}{4} & 0 \\ 0 & 0 & 0 & 0 & 0 & 0 & 0 & 0 & 1 \end{pmatrix} \begin{pmatrix} p_1^n \\ p_1^n \end{pmatrix} = \begin{pmatrix} 0 \\ \mathcal{I} \end{pmatrix} c_0.$$

*Figure 5 depicts the basis functions for Natural Cubic Splines resulting from this solution process. They are the solutions to the above system where interpolation is enforced over the knots  $T_0 = \{0, 1, 2, 3, 4\}$  and the interpolation conditions  $c_0$  are a unit vectors of the form  $(0, \dots, 0, 1, 0, \dots, 0)$ .*

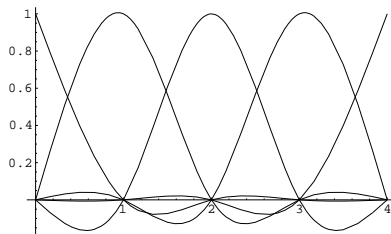


Fig. 5. Interpolating basis for natural cubic splines as yielded by the interpolating finite element process.

*The piecewise Bézier representations  $F_k(t)$  converge to a minimizer of the variational problem by theorem 11. Furthermore, the coefficient vectors  $p_k$  converge to the functions  $F_k(t)$  according to De Boor [dB72b] pp. 154. As a result, the coefficient vectors  $p_k$  themselves converge to a minimizer of the variational problem as  $k \rightarrow \infty$ .*

## 2.4 Minimization with Interpolated Differences

This section applies a change of basis to the just introduced interpolating finite element process. Using a re-formulation of (13) to an approximating solution, we concisely characterize subdivision schemes that converge to minimizers of elliptic, self-adjoint variational problems.

The second row of the system (13) determines  $p_k$  such that  $F_k(t) = B_k(t)p_k$  interpolates  $c_0$  over  $T_0$ . Unfortunately, in many cases this interpolation leads to undesirable properties of the solution  $p_k$ . For example, changing just one of the entries in  $c_0$  for Natural Cubic Splines results in a global change in the solution. This section presents a new scheme which leads to solutions with much nicer properties.

To this effect, we apply a change of basis transformation to the interpolating finite element problem (13): The interpolation conditions are replaced by constraints on the energy of the solution. Equation (13) can be rephrased as

$$\begin{pmatrix} E_k^{\text{uu}} & E_k^{\text{un}} \\ E_k^{\text{nu}} & E_k^{\text{nn}} \end{pmatrix} \begin{pmatrix} p_k^{\text{u}} \\ p_k^{\text{n}} \end{pmatrix} = \begin{pmatrix} 0 \\ E_0 \end{pmatrix} p_0, \quad (14)$$

where  $p_0$  is some initial set of control points centered over the initial knots  $T_0$ . Note that (14) forces the  $p_k$  to be chosen such that those differences in  $E_k p_k$  centered over the knots  $T_0$  are the same as the original differences at these knots, i.e.  $E_0 p_0$ . All remaining entries in  $E_k p_k$  must be zero.

To see that the interpolating and approximating finite element processes are related by a change of basis, we first have to expose the respective bases. To this end, the interpolating system (13) is expressed as

$$\begin{pmatrix} E_k^{\text{uu}} & E_k^{\text{un}} \\ I_k^{\text{u}} & I_k^{\text{n}} \end{pmatrix} C_k = \begin{pmatrix} 0 \\ \mathcal{I} \end{pmatrix}, \quad (15)$$

where  $C_k$  is a solution matrix whose columns contain the coefficients of the interpolating *cardinal basis* functions  $B_k(t)C_k$  of level  $k$ . Similarly, the approximating finite element process (14) is rewritten as a matrix problem

$$\begin{pmatrix} E_k^{\text{uu}} & E_k^{\text{un}} \\ E_k^{\text{nu}} & E_k^{\text{nn}} \end{pmatrix} N_k = \begin{pmatrix} 0 \\ E_0 \end{pmatrix}, \quad (16)$$

where the columns of the solution  $N_k$  contain the coefficients of *approximating basis* functions  $B_k(t)N_k$  for the problem. The following theorem shows that the columns of  $N_k$  are linear combinations of columns of  $C_k$ .

**Theorem 13** *The cardinal basis  $C_k$  and the approximating basis  $N_k$  are related by a change of basis, i.e.*

$$N_k = C_k M_k$$

for some matrix  $M_k$ .

**Proof:** Recall that  $C_k$  was defined as a solution to (15), i.e.

$$\begin{pmatrix} E_k^{\text{uu}} & E_k^{\text{un}} \\ I_k^{\text{u}} & I_k^{\text{n}} \end{pmatrix} C_k = \begin{pmatrix} 0 \\ \mathcal{I} \end{pmatrix},$$

while  $N_k$  was defined as a solution to (16), i.e.

$$\begin{pmatrix} E_k^{\text{uu}} & E_k^{\text{un}} \\ E_k^{\text{nu}} & E_k^{\text{nn}} \end{pmatrix} N_k = \begin{pmatrix} 0 \\ E_0 \end{pmatrix}.$$

According to the first row of (15),  $(E_k^{\text{uu}} \ E_k^{\text{un}}) C_k = 0$ , the columns of  $C_k$  lie in the nullspace of  $(E_k^{\text{uu}} \ E_k^{\text{un}})$ . In fact,  $C_k$  spans the nullspace of  $(E_k^{\text{uu}} \ E_k^{\text{un}})$  because  $\begin{pmatrix} E_k^{\text{uu}} & E_k^{\text{un}} \\ I_k^{\text{u}} & I_k^{\text{n}} \end{pmatrix}$  is invertible and because the columns of  $\begin{pmatrix} 0 \\ \mathcal{I} \end{pmatrix}$  are linear independent.

However, by the first row of (16),  $(E_k^{\text{uu}} \ E_k^{\text{un}}) N_k = 0$ , the columns of  $N_k$  lie in the nullspace of  $(E_k^{\text{uu}} \ E_k^{\text{un}})$  as well. Therefore, the columns of  $N_k$  can be expressed as a linear combination of the columns of  $C_k$ . The change of basis matrix  $M_k$  contains the weights for expressing columns of  $N_k$  in terms of a linear combination of the columns of  $C_k$ .  $\square$

The  $C_k$  converge to a basis for the space of minimizers for the variational problem due to theorem 11. By theorem 13, the columns of  $N_k$  can be expressed as linear combinations of the columns of  $C_k$ . Finally, by theorem 3, the space of minimizers of the variational problem is linear. Thus, if the  $N_k$  converge, then they converge to minimizers of the variational problem as well.

At this point, establishing convergence of  $N_k$  can be reduced to showing convergence of the change of basis matrices  $M_k$  — which is well beyond the scope of this paper. We rather derive subdivision schemes for the approximating basis functions  $N_k$ . If necessary, convergence of the subdivision scheme can be shown using standard techniques [Rei95,Zor98]. Once convergence of the subdivision scheme is established we thus know by the combination of theorems 3, 11, and 13 that the scheme has to converge to minimizers of the variational problem.

Reverting the block decomposition, (14) can be expressed more concisely as

$$\begin{pmatrix} E_k^{uu} & E_k^{un} \\ E_k^{nu} & E_k^{nn} \end{pmatrix} \begin{pmatrix} p_k^u \\ p_k^n \end{pmatrix} = E_k p_k = \begin{pmatrix} 0 \\ E_0 \end{pmatrix} p_0 \quad (17)$$

The right-hand side of (17) can be expressed more concisely using the notion of an upsampling matrix  $U_{k-1}$  which replicates coefficients associated with knots in  $T_{k-1}$  to the next finer grid  $T_k$  and forces zero coefficients at the knots  $T_k - T_{k-1}$ . Now (14) can be restated as

$$E_k p_k = U_{k-1} U_{k-2} \cdots U_0 E_0 p_0. \quad (18)$$

Again, equation (18) states that the  $p_k$  are chosen such that  $E_k p_k$  reproduces the differences  $E_0 p_0$  over the original knots  $T_0$  and forces zero differences at all knots in  $T_k - T_0$ .

**Example 14** *The upsampling matrix  $U_0$  which carries coefficients over knot set  $T_0 = \{0, 1, 2, 3, 4\}$  to coefficients over the knot set  $T_1 = \{0, \frac{1}{2}, 1, \frac{3}{2}, 2, \frac{5}{2}, 3, \frac{7}{2}, 4\}$  is given by*

$$U_0 = \begin{pmatrix} 1 & 0 & 0 & 0 & 0 \\ 0 & 0 & 0 & 0 & 0 \\ 0 & 1 & 0 & 0 & 0 \\ 0 & 0 & 0 & 0 & 0 \\ 0 & 0 & 1 & 0 & 0 \\ 0 & 0 & 0 & 0 & 0 \\ 0 & 0 & 0 & 1 & 0 \\ 0 & 0 & 0 & 0 & 0 \\ 0 & 0 & 0 & 0 & 1 \end{pmatrix}.$$

*The matrix multiplication  $v_1 = U_0 v_0$  for some  $v_0$  of size 5 yields a coefficient vector  $v_1$  of size 9.  $v_1$  contains the values from  $v_0$  for the knots  $T_0$ , and value 0 for all remaining knots.*

Two such conditions (18) for levels  $k$  and  $k + 1$  can be assembled as

$$\begin{aligned} E_k p_k &= U_{k-1} \cdots U_0 E_0 p_0 \\ E_{k+1} p_{k+1} &= U_k \cdots U_0 E_0 p_0. \end{aligned}$$

Combining them yields  $E_{k+1} p_{k+1} = U_k E_k p_k$ . Finally, applying the definition of the subdivision matrix,  $p_{k+1} = S_k p_k$ , yields the fundamental relationship

$$\boxed{E_{k+1} S_k = U_k E_k.} \quad (19)$$

Note that equation (19) allows us to express the solution to the variational problem as a subdivision scheme defined by the subdivision matrices  $S_k$ .

The behavior of the associated subdivision scheme is clear.  $S_k$  places the new control points  $p_{k+1}$  so as to replicate the differences  $E_k p_k$  over the old knots  $T_k$  and forces differences at the new knots  $T_{k+1} - T_k$  to be zero.

**Example 15** We can use the piecewise quadratic Bézier curves described in example 9 as the finite element basis  $B_1(t)$  in our derivation of the energy matrix  $E_1$  for (7). Consequently,  $E_1$  has rows that are multiples of the sequence  $\{\dots, 0, 1, -4, 6, -4, 1, 0, \dots\}$ . Applying this mask to  $S_0$  from the Lane-Riesenfeld algorithm (Example 8) yields the matrix  $E_1 S_0$  whose rows alternate between all zeroes and rows that are multiples of  $\{\dots, 0, 1, -4, 6, -4, 1, 0, \dots\}$ . Hence, the action of  $S_0$  is to position the new control points  $p_1 = S_0 p_0$  such that  $E_1 p_1$  replicates the differences of the original differences  $E_0 p_0$  at the knots of  $T_0$  and forces zero differences at new knots in  $T_1 - T_0$ . Figure 6 illustrates this idea.

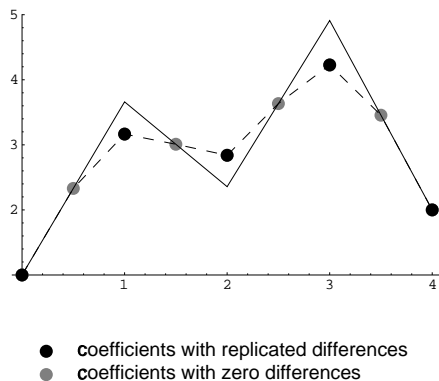


Fig. 6. Coefficients shaded by difference type.

Note that the resulting subdivision scheme is not necessarily interpolating. To insure interpolation, the initial control points  $p_0$  must be chosen such that the limit interpolates the desired values over  $T_0$ .

**Example 16** For Natural Cubic Splines, the columns of  $E_{k+1}$  are not linearly independent and equation (19) does not uniquely determine  $S_k$ . However, enforcing minimal support of  $S_k$  yields a unique solution.

By equation (19), the subdivision matrix  $S_0$  satisfies the equation  $E_1 S_0 = U_0 E_0$ ,

$$8 \begin{pmatrix} 1 & -2 & 1 & 0 & 0 & 0 & 0 & 0 & 0 \\ -2 & 5 & -4 & 1 & 0 & 0 & 0 & 0 & 0 \\ 1 & -4 & 6 & -4 & 1 & 0 & 0 & 0 & 0 \\ 0 & 1 & -4 & 6 & -4 & 1 & 0 & 0 & 0 \\ 0 & 0 & 1 & -4 & 6 & -4 & 1 & 0 & 0 \\ 0 & 0 & 0 & 1 & -4 & 6 & -4 & 1 & 0 \\ 0 & 0 & 0 & 0 & 1 & -4 & 6 & -4 & 1 \\ 0 & 0 & 0 & 0 & 0 & 1 & -4 & 5 & -2 \\ 0 & 0 & 0 & 0 & 0 & 0 & 1 & -2 & 1 \end{pmatrix} S_0 = \begin{pmatrix} 1 & -2 & 1 & 0 & 0 \\ 0 & 0 & 0 & 0 & 0 \\ -2 & 5 & -4 & 1 & 0 \\ 0 & 0 & 0 & 0 & 0 \\ 1 & -4 & 6 & -4 & 1 \\ 0 & 0 & 0 & 0 & 0 \\ 0 & 1 & -4 & 5 & -2 \\ 0 & 0 & 0 & 0 & 0 \\ 0 & 0 & 1 & -2 & 1 \end{pmatrix}.$$



From this characterization it becomes clear that any solution for the Natural Cubic Spline variational problem has to satisfy the “natural” boundary conditions of having second derivative zero at both endpoints: The first and last row in both energy matrices above measure the second difference next to the endpoint of the spline. However, these differences scale by a factor of  $\frac{1}{8}$  between the left and right-hand side of the equation. Thus, as  $k \rightarrow \infty$ , this difference converges to zero.

Since  $E_1$  is not invertible,  $S_0$  is not uniquely determined. Ideally, we would like subdivision rules that agree with those for cubic B-Splines on the interior of  $\Omega$  and are local on the boundary of  $\Omega$ . Luckily, such an  $S_0$  exists and has the form:

$$S_0 = \frac{1}{8} \begin{pmatrix} 8 & 0 & 0 & 0 & 0 \\ 4 & 4 & 0 & 0 & 0 \\ 1 & 6 & 1 & 0 & 0 \\ 0 & 4 & 4 & 0 & 0 \\ 0 & 1 & 6 & 1 & 0 \\ 0 & 0 & 4 & 4 & 0 \\ 0 & 0 & 1 & 6 & 1 \\ 0 & 0 & 0 & 4 & 4 \\ 0 & 0 & 0 & 0 & 8 \end{pmatrix}.$$

These rules agree with the rules for uniform cubic subdivision on the interior of  $\Omega$  and are local at the boundary of  $\Omega$ . Subsequent subdivision matrices  $S_k$  have the same structure.

Remarkably, the resulting splines are piecewise cubic functions, even at the boundary of  $\Omega$ . These subdivision rules for the endpoints of a cubic B-Spline were proposed previously by DeRose et al. in [HDD<sup>+</sup>94]. However, the authors derived the rules in an ad hoc manner and failed to recognize their interesting properties.

### 3 Variational Splines Over Uniform Knot Sequences

In this section, we examine two variational problems over the simplest type of knot sequences, uniform knots. If the domain  $\Omega$  is  $\mathbb{R}^d$ , then these uniform knot sequences  $T_k$  are dilates of the integer grid  $\mathbb{Z}^d$ ,

$$T_k = \frac{1}{2^k} \mathbb{Z}^d.$$

In the first example, we derive the subdivision rules for B-Splines from their corresponding variational problem. In the second example, we derive subdivision rules for splines that satisfy the harmonic equation, also known as Laplace’s equation. Throughout this section we will use generating functions as a convenient and concise way of representing sequences of coefficients. The reader unfamiliar with gen-

erating functions is referred to Dyn [Dyn92] which discusses their use for subdivision in great depth.

### 3.1 B-Splines

The uniform B-Splines of order  $2m$  are defined over the real line  $\mathbb{R}$  (the domain  $\Omega$ ) and minimize the energy functional  $\mathcal{E}$ , as defined in (4), whose associated differential operator  $\mathcal{D}$  is of order  $m$ , i.e.

$$\mathcal{D} = \frac{\partial^m}{\partial t^m}.$$

We next derive the subdivision rules for these B-Splines using a variational approach.

We choose the finite element basis functions  $B_k(t)$  to be uniform B-Splines of degree  $m$  (i.e. order  $m + 1$ ). For even  $m$ , these basis functions are then translated by a factor of  $2^{-k-1}$  to center the basis functions over the knots  $T_k$  such that exactly one of the basis functions has maximal magnitude over any knot.

Application of the  $m$ th derivative operator  $\mathcal{D}$  to the B-spline finite element representation  $F_k(t) = B_k(t)p_k$  yields  $\mathcal{D}F_k(t) = \mathcal{D}(B_k(t)p_k)$ . Because the  $m$ th derivative of a degree  $m$  B-spline can be written as a degree  $m - m$ , i.e. piecewise constant B-spline, we get  $\mathcal{D}B_k(t) = D_k \hat{B}_k(t)$  where  $D_k$  is a matrix of discrete differences and  $\hat{B}_k(t)$  are the piecewise constant B-spline basis functions over the knots  $T_k$  [Far88].

In the uniform case, all of the matrices  $D_k$  have rows that are all shifts and multiples of a single fundamental sequence. The coefficients of this sequence can be conveniently captured by the generating function  $d(z)$  where

$$d(z) = (1 - z)^m.$$

Because the inner product  $\int \hat{b}_k^i(t)\hat{b}_k^j(t)$  of the  $i$ th and  $j$ th piecewise constant B-spline basis function in  $\hat{B}_k(t)$  is one if  $i = j$  and zero otherwise, the energy of  $F_k(t)$ ,  $\mathcal{E}[F_k]$  is given by  $p_k^T D_k^T D_k p_k$ . Accordingly, the rows of the corresponding energy matrices  $D_k^T D_k$  are all shifts and multiples of a single fundamental sequence  $e(z)$  given by

$$e(z) = d\left(\frac{1}{z}\right)d(z).$$

The usefulness of expressing  $e(z)$  in terms of a generating function is that the corresponding subdivision matrices can also be expressed in terms of generating functions.

In the uniform case, the columns of the subdivision matrices  $S_k$  can be chosen to be shifts of a single sequence. The generating function  $s(z)$  for this sequence encodes the coefficients of  $S_k$  as follows: the  $ij$ th entry of  $S_k$  is  $s_{i-2j}$ . Rewriting equation (19) in terms of generating functions yields

$$2^{2m}e(z)s(z) = 2e(z^2). \quad (20)$$

$e(z^2)$  reflects the action of the upsampling matrices  $U_k$  on  $E_k$ . The factor of  $2^{2m}$  reflects the effect of halving the knot spacing on  $\mathcal{D}$ . The factor of 2 of the right-hand side reflects the effect of halving the knot spacing on the integral.

Recalling that  $d(z) = (1 - z)^m$ , then

$$e(z) = \left(1 - \frac{1}{z}\right)^m (1 - z)^m$$

Since  $1 - z$  divides  $1 - z^2$ ,  $e(z)$  must divide  $e(z^2)$ . Therefore,

$$s(z) = \frac{(1 + z)^{2m}}{2^{2m-1} z^m}$$

by equation (20). This generating function encodes the subdivision rules for a B-Spline of order  $2m$  (degree  $2m - 1$ ) [LR80]. For example, the generating function  $s(z)$  for uniform cubic B-Spline subdivision is

$$\frac{(1 + z)^4}{8z^2} = \frac{1}{8} \left(1z^{-2} + 4z^{-1} + 6 + 4z^1 + 1z^2\right).$$

### 3.2 Harmonic Splines

Let the domain  $\Omega$  be the real plane,  $\mathbb{R}^2$ . Consider the energy functional

$$\mathcal{E}[F] = \int_{\Omega} \left(\frac{\partial}{\partial t_1} F(t)\right)^2 + \left(\frac{\partial}{\partial t_2} F(t)\right)^2 dt$$

where  $t = (t_1, t_2)$ . The Euler Lagrange Theorem yields the *harmonic equation*:

$$\frac{\partial^2}{\partial t_1^2} F(t) + \frac{\partial^2}{\partial t_2^2} F(t) = 0.$$

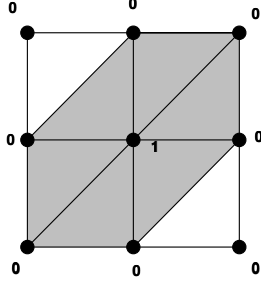


Fig. 7. A piecewise linear finite element basis.

We refer to the functions that satisfy this equation as harmonic splines. We next derive a set of subdivision rules for harmonic splines over uniform grids.

The knot sets  $T_k$  partition  $\Omega$  into a square grid. If each square is split into two triangles, the piecewise linear hat functions for this grid form a suitable finite element basis  $B_k(t)$  (see figure 7). There are two ways to split the square grid into triangles. However, the resulting energy matrices are independent of the actual split chosen.

As before, the rows of the energy matrices  $E_k$  are all multiples and shifts (in the two-dimensional grid) of a fundamental sequence  $e(z)$ . If  $d_1(z)$  and  $d_2(z)$  are the discrete analogs of  $\frac{\partial}{\partial t_1}$  and  $\frac{\partial}{\partial t_2}$ , then

$$\begin{aligned} d_1(z) &= (1 - z_1) \\ d_2(z) &= (1 - z_2) \end{aligned}$$

where  $z = (z_1, z_2)$ . The energy mask  $e(z)$  satisfies

$$e(z) = d_1(z)d_1\left(\frac{1}{z}\right) + d_2(z)d_2\left(\frac{1}{z}\right).$$

Plotting the coefficients  $e_{ij}$  of  $e(z)$  at  $(i, j) \in \{-1, 0, 1\}^2$  yields the two-dimensional energy mask

$$\begin{array}{ccc} & -1 & \\ -1 & 4 & -1 \\ & -1 & \end{array}$$

The generating function  $s(z)$  for the associated subdivision scheme satisfies a generalization of equation (20)

$$2^{2m} e(z)s(z) = 2^d e(z^2).$$

The factor of  $2^d$  reflects the effect of halving the knot spacing on the integral in  $\mathcal{E}$ . In the case of harmonic splines,  $m = 1$  and  $d = 2$  so the subdivision mask  $s(z)$  is simply  $\frac{e(z^2)}{e(z)}$ . For B-Splines,  $e(z)$  exactly divides  $e(z^2)$  and the resulting subdivision rules were finite. For harmonic splines,  $e(z)$  does not exactly divide  $e(z^2)$ . Fortunately,  $s(z)$  still exists as a bi-infinite power series. To generate this series, we use the expansion of  $\frac{e(z^2)}{e(z)}$  as a bi-infinite power series in the neighborhood of  $z = 1$  (i.e. the Laurent expansion).

At first glance, this expansion may appear to be ill-defined since  $e(1) = 0$ . However, as we next show,  $s(z)$  is well-defined in the neighborhood of  $z = 1$ . The behavior of  $s(z)$  at  $z = 1$  is equivalent to that of  $s(1 - \hat{z})$  at  $\hat{z} = 0$ . Substituting  $1 - \hat{z}$  into  $e(z)$  yields

$$\begin{aligned} e(1 - \hat{z}) &= \frac{\hat{z}_1^2}{1 - \hat{z}_1} + \frac{\hat{z}_2^2}{1 - \hat{z}_2} \\ &= \frac{\hat{z}_1^2 + \hat{z}_2^2 + O(\hat{z}^3)}{(1 - \hat{z}_1)(1 - \hat{z}_2)} \end{aligned}$$

Substituting this expansion and a similar expansion for  $e((1 - \hat{z})^2)$  into equation (20) yields

$$s(1 - \hat{z}) = \frac{4\hat{z}_1^2 + 4\hat{z}_2^2 + O(\hat{z}^3)}{\hat{z}_1^2 + \hat{z}_2^2 + O(\hat{z}^3)}.$$

In this form, two important properties of  $s(1 - \hat{z})$  become clear. First,  $s(1 - \hat{z})$  is convergent at  $\hat{z} = 0$ . Second,  $s(1 - \hat{z})$  is defined for some open neighborhood of  $\hat{z} = 0$  since  $\hat{z}_1^2 + \hat{z}_2^2$  vanishes only at  $\hat{z} = 0$ .

Figure 8 gives a two-dimensional plot of a subset of the bi-infinite coefficient mask encoded by  $s(z)$ . Note that these coefficients decay very rapidly as  $|z| \rightarrow \infty$ . Due to this fast decay, the exact subdivision matrix  $S$  can be approximated to a high precision by a sparse subdivision matrix  $\hat{S}$ . Section 4.1 discusses a systematic method for constructing such an approximation.

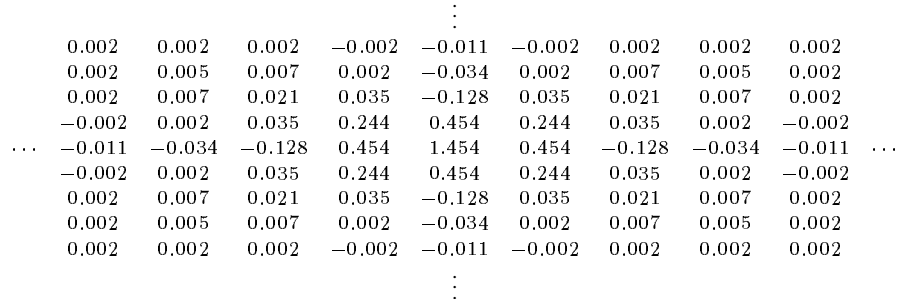


Fig. 8. Plot of the coefficients of  $s(z)$  for harmonic splines.

An application of this subdivision scheme is shown in figure 9. Starting in the upper left we depict in clockwise order the control grid after 0, 1, 2, and 3 applications of the subdivision matrix  $S$ .

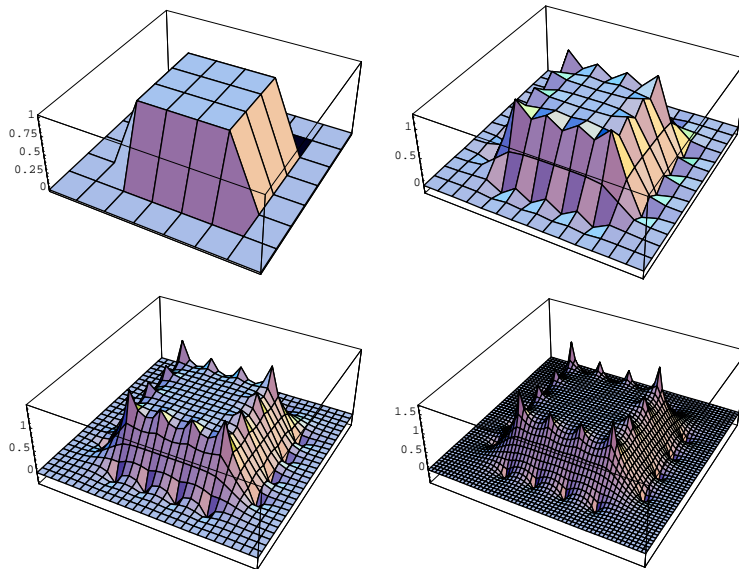


Fig. 9. Example application of the subdivision scheme for harmonic splines.

Again, by theorem 11 the interpolating finite element solver for harmonic splines converges to the true minimizer of the variational problem because the piecewise linear finite element functions completely span the linear polynomials and because the aspect ratio of the two dimensional elements (domain triangles) is bounded by a constant at any level. As before, a simple change of basis links the approximating subdivision scheme and the interpolating finite element solver. Thus, the approximating subdivision scheme  $s(z)$  for harmonic splines also converges to minimizers of the variational problem. In fact, because the underlying finite element basis were piecewise linear hat functions, the coefficients themselves converge to the minimizer of the variational problem.

As a quick side note, if we let

$$\nabla = \frac{\partial^2}{\partial t_1^2} + \frac{\partial^2}{\partial t_2^2},$$

then  $\nabla F(t) = 0$  is the harmonic (or Laplace's) equation.

## 4 Subdivision Schemes for Bounded Knot Sequences

In this section, we consider a situation of practical importance. How do these uniform subdivision schemes behave if the domain  $\Omega$  is bounded? As we shall see, the resulting subdivision schemes have rules that vary depending on their relation to the boundary of  $\Omega$ . However, the resulting rules are still independent of the level of subdivision.

### 4.1 Harmonic Splines

We consider the variational problem of harmonic splines. In this case, we bound the domain  $\Omega$  to be the square  $[0, 4]^2$ . Our approach to this problem consists of three steps:

- Choose a sequence of finite element bases  $B_k(t)$  and derive a corresponding sequence of energy matrices  $E_k$ .
- Given these energy matrices  $E_k$ , derive exact, globally supported subdivision rules  $S_k$  satisfying

$$E_{k+1}S_k = U_k E_k.$$

- Approximate these exact subdivision rules of  $S_k$  by a finite set of locally supported subdivision rules  $\hat{S}_k$ .

We next describe each of these steps.

#### 4.1.1 Finite Element Bases and Energy Matrices

Figure 7 depicted the canonical finite element for harmonic splines whose integer translates form a basis for the solution space. Restricting the support of these elements to  $\Omega$  yield the desired set of bases  $B_k(t)$ . Note that there are only three types of elements; interior elements, boundary elements and corner elements.

The corresponding energy matrices  $E_k$  have a similar structure.  $E_k$  contains only three types of rows; interior rows, edge rows and corner rows. Each type of row has a single canonical mask associated with it. Figure 10 illustrates this property for  $E_0$ .

#### 4.1.2 Constructing the Exact Subdivision Rules

Since the energy matrices  $E_k$  are not invertible, equation (19) does not uniquely determine an associated subdivision scheme. In particular, equation (19) does not

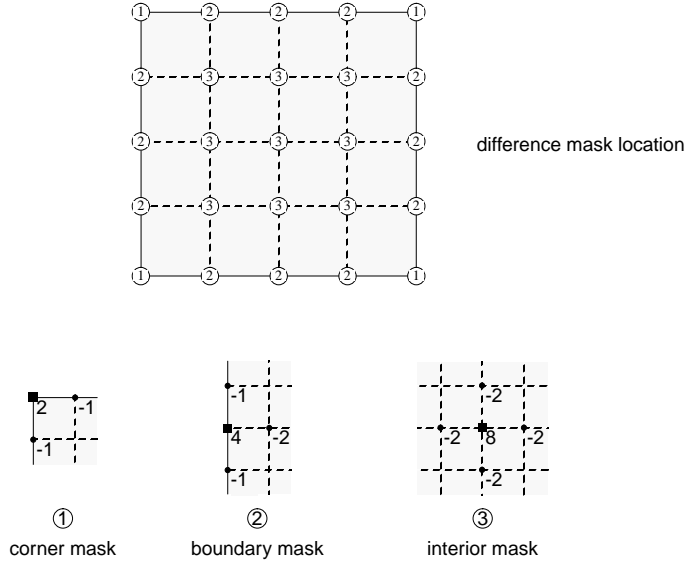


Fig. 10. Rows of energy matrices for bounded harmonic splines specify the action of the subdivision scheme on the constant function one.

To this purpose, let  $M_k$  denote integrals of the basis functions  $B_k(t)$ ,

$$M_k = \int_{\Omega} B_k(t) dt.$$

For example, the entries of  $M_0$  are either 1,  $\frac{1}{2}$ , or  $\frac{1}{4}$  depending on whether the corresponding basis function lies in the interior, on a boundary, or at a corner of  $\Omega$ . By the linearity of integration,  $M_k p_k$  is exactly the integral of  $F_k(t) = p_k B_k(t)$ . If we add the restriction that the subdivision scheme preserve the integrals of the finite element approximations, then

$$M_{k+1} p_{k+1} = M_{k+1} S_k p_k = M_k p_k.$$

Since this condition holds for all  $p_k$ ,  $S_k$  satisfies

$$M_{k+1} S_k = M_k.$$

With this added equation,  $S_k$  is uniquely determined. If the  $B_k(t)$  form a partition of unity, then  $S_k$  has constant precision.

The resulting subdivision matrices  $S_k$  have two interesting properties.

- The subdivision rules comprising  $S_k$  have a very localized influence. The value of a coefficient on  $T_{k+1}$  depends mainly on a few nearby coefficients in  $T_k$ . This property follows directly from the fact that the  $S_k$  are derived from a variational



problem. Non-local influence would be inconsistent with a low “energy” solution to the variational problem.

- The subdivision matrices  $S_k$  are converging to a single subdivision matrix  $S$  in the neighborhood of a corner of  $\Omega$ . This property is due to the fact that the knot grids  $T_k$  are locally dilates of each other at the corners of  $\Omega$ . As a result, the effect of  $S_k$  can be approximated by a set of rules that are independent of  $k$ .

#### 4.1.3 Finite Approximation of the Exact Subdivision Rules

Based on these two observations, we suggest approximating these exact subdivision rules by a finite collection of compactly supported subdivision rules. In particular, we propose using 10 distinct types of subdivision rules; three rules at the corners of  $\Omega$ , four rules along the boundaries of  $\Omega$  and three rules for the interior of  $\Omega$ . Figure 11 illustrates location of these 10 rules on a five by five grid of knots.

To compute these rules, we treat them as unknowns with the same support as those for a bi-cubic B-Spline and denote the resulting subdivision matrices  $\hat{S}_k$ . Our goal is to compute values for the unknown entries of  $\hat{S}_k$  such that

$$E_{k+1}\hat{S}_k \approx U_k E_k.$$

More precisely, we wish minimize the expression

$$\min_{\hat{S}_k} \|E_{k+1}\hat{S}_k - U_k E_k\|_{\infty}. \quad (21)$$

Recall that the infinity norm of a matrix is the maximum over all rows of the sum of absolute values of the entries in a given row. Due to the repetition of difference rules in  $E_k$  and the use of only 10 distinct subdivision rules in  $\hat{S}_k$ , there are only 15 distinct rows sums in  $E_{k+1}\hat{S}_k - U_k E_k$  for *any* choice of  $k$ . Three distinct rows sums arise from the unknown interior rules for  $\hat{S}_k$ . 7 and 5 distinct rows sums arise from the special boundary and corner rules of  $\hat{S}_k$ .

The most important consequences of this observation is that the minimizer for expression 21 is also independent of  $k$ . Setting  $k = 0$ , expression 21 can be minimized using linear programming. Figure 11 gives the suggested values for these rules. These rules have also been additionally constrained to have constant precision. The result is a subdivision scheme that approximates the solution to the harmonic equation.

The upper portion of figure 12 is an initial five by five grid of control points. The lower left portion of the figure is a 17 by 17 grid produced by applying the exact subdivision scheme for harmonic splines to this initial grid. This surface was computed via matrix inversion. The lower right portion is the 17 by 17 grid produced

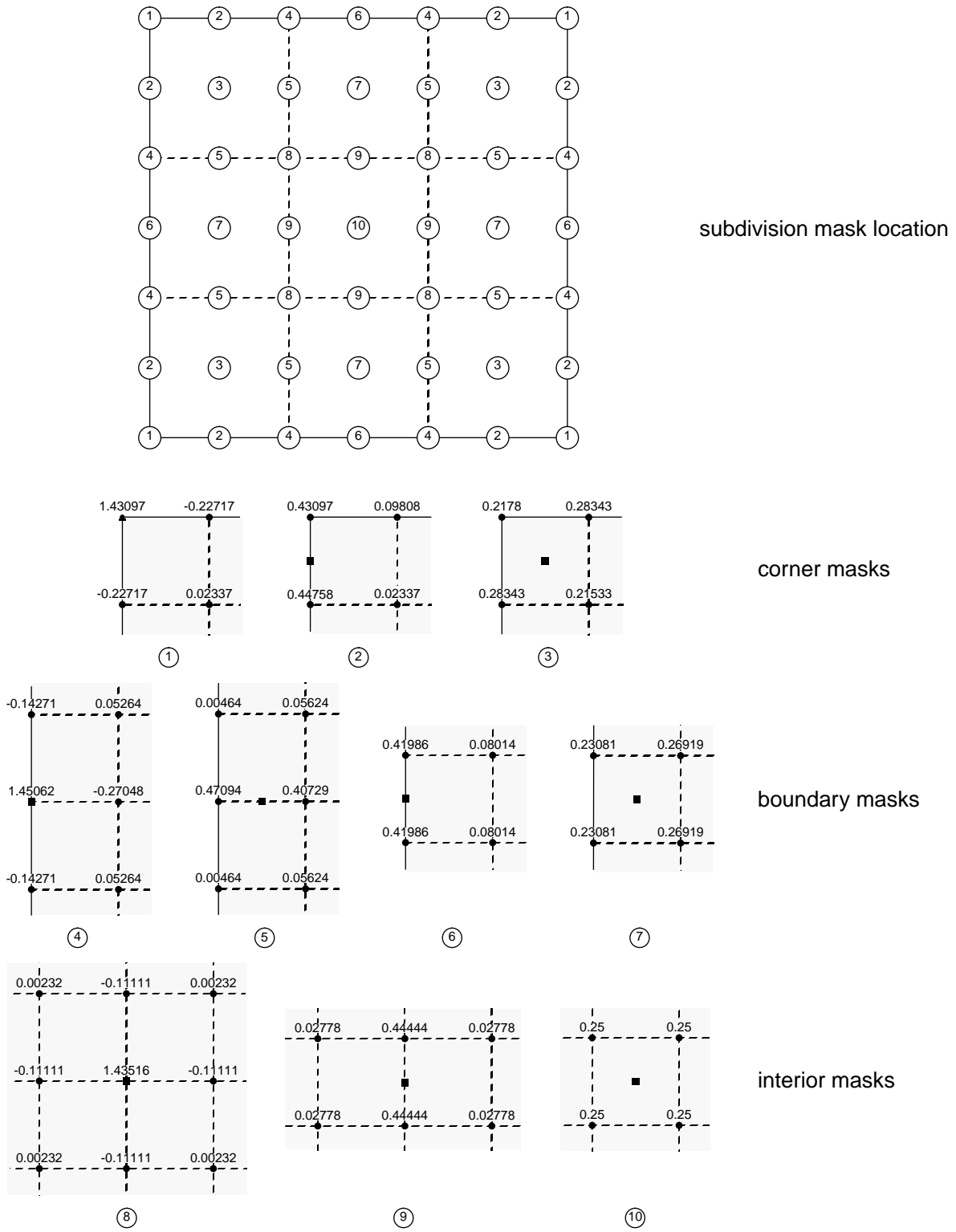


Fig. 11. Finite subdivision rules for bounded harmonic splines

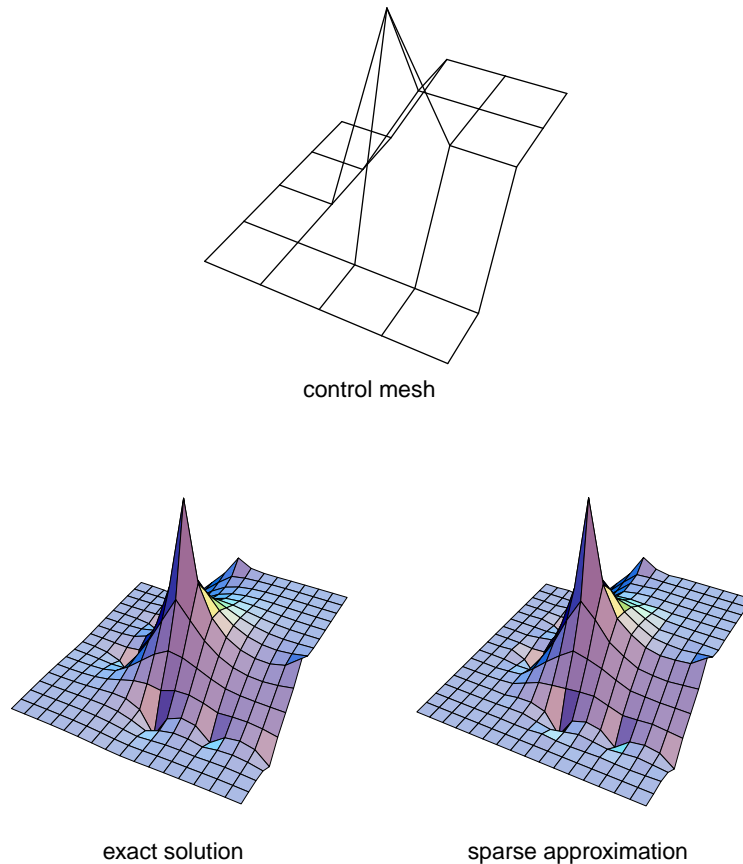


Fig. 12. An example of subdivision for bounded harmonic splines

by applying the local rules of figure 11. For those who wish, a Mathematica implementation of these computations for harmonic splines is available as a technical report [WW97].

## 5 Conclusions and Future work

We showed that an important class of variational problems has a fundamental nesting property of the related solution spaces. Modifying the traditional finite element solution process to utilize interpolation of energy values instead of function values, we were able to derive a concise characterization of subdivision schemes that capture this nesting to express finer and finer solutions to these variational problems. While the exact solution in many cases requires a globally supported subdivision scheme, a locally supported and stationary scheme can be used to approximate the solution to a high degree of accuracy.

The results of this paper lead to a variety of interesting problems. Here are several possibilities for future work identified by the authors.

### 5.1 *Interpolation with Approximating Subdivision Schemes*

The subdivision schemes derived according to the methodology presented here are approximating, i.e. the limit objects do not go through the original, coarsest control points. Instead, given a set of interpolation conditions  $c_0$  an appropriate set of initial control points  $p_0$  has to be determined first such that the limit interpolates  $c_0$ . For stationary subdivision schemes this problem can be solved very efficiently using an interpolation matrix. This matrix contains samples of the underlying subdivision basis functions at the knots of the coarsest grid and can be derived from the subdivision matrix in a straightforward solution process.

### 5.2 *Locality of the Subdivision Schemes*

In finite element analysis, the energy matrices  $E_k$  depend on the initial choice of the finite element bases  $B_k(t)$ . Different sequences of bases lead to different sequences of energy matrices. According to our analysis, the energy matrices determine a subdivision scheme for the space of minimizers. Different set of energy matrices leads to different subdivision scheme for the *same* space of minimizers. The fundamental problem here is determining the set of energy matrices that maximize the “locality” of the corresponding subdivision scheme.

### 5.3 *Multi-Resolution Methods for Variational Problems*

Variational subdivision and multi-resolution analysis are intrinsically linked. We intend to explore this idea in terms of determining a “natural” wavelet basis associated with the subdivision scheme. Another interesting problem involves applying multi-grid corrections to the local rules used in approximating the globally supported, exact subdivision schemes. The user could apply the local subdivision rules as desired with the option of applying a multi-grid correction when necessary.

### 5.4 *Subdivision Schemes for Thin Plate Splines*

We have purposefully left the most interesting variational problem, that of Thin Plate Splines, to another paper. The finite element bases necessary to create a subdivision scheme for these splines are rather involved and deserve a complete exposition. Using these bases, equation (19) is employed to derive subdivision schemes for several important cases including

- regular subdivision of bounded, rectangular grids [WW98],

- regular subdivision of irregular, triangular grids.

### 5.5 Knot Insertion Schemes for Irregular Data

Subdivision schemes insert many different knots simultaneously. Knot insertion schemes insert a single knot at a time. Remarkably, equation (19) can be used to derive knot insertion algorithms for variational problems. In a second paper [War97], we show that Boehm's algorithm for knot insertion into B-Splines can be derived directly from equation (19). The key to this construction is that divided differences can be captured as the solution to a very simple problem in linear algebra. The paper concludes by developing a knot insertion algorithm for harmonic splines.

### Acknowledgments

This work has been supported in part under National Science Foundation grants number CCR-9500572 and CCR-9732344, Texas Advanced Technology Program grant number 003604-010 and by Western Geophysical.

The authors would like to thank the anonymous reviewers for their constructive comments which greatly helped improve the quality of the paper.

### References

- [Boe80] W. Boehm. Inserting new knots into B-spline surfaces. *Computer-aided Design*, 12:99–102, 1980.
- [dB72a] Carl de Boor. On calculating with B-splines. *Journal of Approximation Theory*, 6:50–62, 1972.
- [dB72b] Carl de Boor. *A Practical Guide to Splines*. Springer-Verlag, 1972.
- [Dyn86] Nira Dyn. Numerical procedures for surface fitting of scattered data by radial functions. *SIAM J. Sci. Stat. Comput.*, 7(2):639–659, 1986.
- [Dyn87] Nira Dyn. Interpolation of scattered data by radial functions. In C. K. Chui, L. L. Schumaker, and F. I. Utreras, editors, *Topics in Multivariate Approximation*, pages 47–61. Academic Press, 1987.
- [Dyn92] Nira Dyn. Subdivision schemes in computer aided geometric design. In W. Light, editor, *Advances in Numerical Analysis II*, pages 36–104. Oxford University Press, 1992.

- [Far88] Gerald Farin. *Curves and Surfaces for Computer Aided Geometric Design: A Practical Guide*. Academic Press Inc., New York, 1988.
- [HDD<sup>+</sup>94] H. Hoppe, T. DeRose, T. Duchamp, M. Halstead, H. Jin, J. McDonald, J. Schweitzer, and W. Stuetzle. Piecewise smooth surface reconstruction. *Computer Graphics*, 28:295–302, 1994.
- [HL93] J. Hoschek and D. Lasser. *Fundamentals of Computer Aided Geometric Design*. A K Peters, 1993.
- [KCVS98] Leif Kobbelt, Sven Campagna, Jens Vorsatz, and Hans-Peter Seidel. Interactive multi-resolution modeling on arbitrary meshes. In *SIGGRAPH 98 Conference Proceedings*, Annual Conference Series, pages 105–114, 1998.
- [Kob96] Leif Kobbelt. A variational approach to subdivision. *Computer Aided Geometric Design*, 13:743–761, 1996.
- [KS97] L. Kobbelt and P. Schröder. Constructing variationally optimal curves through subdivision. Technical Report 97-05, California Institute of Technology, Department of Computer Science, 1997.
- [LR80] J. M. Lane and R. F. Riesenfeld. A theoretical development for the computer generation and display of piecewise polynomial surfaces. *IEEE Transactions on Pattern Analysis and Machine Intelligence*, 2(1):35–46, January 1980.
- [OR76] J. T. Oden and J. N. Reddy. *An Introduction to the Mathematical Theory of Finite Elements*. John Wiley & Sons, 1976.
- [Rei95] Ulrich Reif. A unified approach to subdivision algorithms near extraordinary points. *Computer Aided Geometric Design*, 12:153–174, 1995.
- [Sha95] V. V. Shaidurov. *Multigrid Methods for Finite Elements*. Kluwer Academic Publishers, 1995.
- [War97] Joe Warren. Local knot insertion schemes. In preparation, 1997.
- [War98] Joe Warren. Mathematical properties of variational subdivision schemes. Technical Report CS-TR-98-325, Rice University, Department of Computer Science, 1998.
- [WW97] Henrik Weimer and Joe Warren. Variational subdivision for laplacian splines. Technical Report CS-TR-97-291, Rice University, Department of Computer Science, 1997.
- [WW98] Henrik Weimer and Joe Warren. Subdivision schemes for thin-plate splines. *Computer Graphics Forum*, 17(3):303–313 & 392, 1998.
- [Zor98] Denis Zorin. Smoothness of stationary subdivision on irregular meshes. Technical Report CSL-TR-98-752, Stanford University, Computer Systems Laboratory, Departments of Electrical and Computer Engineering, Stanford University, Stanford, CA 94305-9040, 1998.